Toxicology in Vitro 60 (2019) 12–18

Contents lists available at ScienceDirect

Toxicology in Vitro

journal homepage: www.elsevier.com/locate/toxinvit

Surface defects reduce Carbon Nanotube toxicity *in vitro*

Hendrik Requardt[a,*], Armin Braun[a], Pablo Steinberg[b], Silke Hampel[c], Tanja Hansen[a]

[a] Fraunhofer Institute for Toxicology and Experimental Medicine, Department of Preclinical Pharmacology and Toxicology, Nikolai-Fuchs-Straße 1, 30625 Hannover, Germany
[b] Max Rubner-Institute, Federal Research Institute of Nutrition and Food, Haid-und-Neu-Str. 9, 76131 Karlsruhe, Germany
[c] Leibniz Institute for Solid State and Materials Research, Helmholtzstraße 20, 01069 Dresden, Germany

ARTICLE INFO

Keywords:
Carbon nanotubes
Cytotoxicity
Reactive oxygen species
Cell cycle arrest
Surface defects

ABSTRACT

The cytotoxicity of two different types of Multi-walled Carbon Nanotubes (MWCNTs) in A549 lung epithelial cells and HepG2 hepatocytes was investigated. One MWCNT still contained iron that was used as a catalyst during production, while the other one had all iron removed in a post-production heat treatment resulting in significantly fewer surface defects. The WST-8 assay was applied to test cell viability. To check the integrity of the cell membrane, we performed the lactate dehydrogenases assay (LDH) and measured the cellular production of reactive oxygen species (ROS). Finally, to examine cell proliferation, we conducted a cell cycle analysis. The results showed a dose- and time-dependent decrease in cell viability for both MWCNTs in both cell types. Moreover, a dose- and time-dependent increase in LDH leakage was detected, thereby indicating a decreased membrane integrity. The production of ROS was significantly increased in the case of the heat-treated MWCNTs. The heat-treated MWCNTs showed significantly stronger adverse effects when compared to the non-treated MWCNTs. Additionally, the heat-treated MWCNTs induced a dose-dependent cell cycle arrest in A549 cells. Both MWCNTs induced a significant cytotoxicity, whereby the heat treatment, leading to a decrease in surface defects, further increased the indicated adverse effects.

1. Introduction

Given the rise in research and development in the field of nanotechnology and new nanomaterials over the last decades, on the one hand increasing concerns regarding the safety of these materials have been expressed (Holsapple et al., 2005; Oberdorster, Oberdorster, and Oberdorster, 2005a; Oberdorster et al., 2005b; Stern and McNeil, 2007). These concerns have also been accompanied by unjustified reports in the media (Wolinsky, 2006). On the other hand, nanomaterials have been widely used in different areas of interest like mechanical engineering (Miyagawa, Misra, and Mohanty, 2005), electrical engineering (Ahn et al., 2006) and medicine (Salata, 2004; Verma, Domb, and Kumar, 2011; Zhang and Webster, 2008). Alongside several other applications in the field of medicine like imaging, biosensors or medical probes, nanomaterials are also used as drug delivery systems (De Jong and Borm, 2008). In addition to several types of nanoparticles like micelles and dendrimers, Carbon Nanotubes (CNTs) have attracted attention for this type of application (Bianco, Kostarelos, and Prato, 2005; Liu et al., 2008a). CNTs are carbon based nanomaterials with unique properties that depend on their structure, diameter, length, and several other attributes. CNTs are mainly divided into two distinct groups, Single-Walled (SW) and Multi-Walled (MW) CNTs. SWCNTs are composed of one single graphene layer furled to a tube, whereas MWCNTs consist of either several tubes stacked into one another or one wide graphene layer furled into a spiral with several walls. Virtually all pristine CNTs show a hydrophobic behavior and can either be conducting or semiconducting. Several processes for producing SW- and MWCNTs utilize iron catalysts, like for example ferrocene gas, to initiate the CNT self-assembly and to enrich CNT yields (Leonhardt et al., 2006; Moisala et al., 2006). Residues of these iron catalysts remain in the produced CNTs and can pose a potential toxicological risk (Aldieri et al., 2013; Kagan et al., 2006; Monteiro-Riviere, Nemanich, Inman, Wang, and Riviere, 2005; Visalli et al., 2017).

In this study, MWCNTs synthesized using chemical vapor deposition with iron (ferrocene) as a catalyst were used. Since residual iron that remains in the tubular structure is a toxicological risk factor, we divided the MWCNTs into two groups. One group was used as produced, containing iron from the catalyst. The other was heat-treated after production to remove all iron from the MWCNTs (see Material and methods). The goal was to investigate the cytotoxicity of these two

* Corresponding author.
E-mail addresses: Requardt.pub@gmail.com (H. Requardt), Armin.Braun@item.fraunhofer.de (A. Braun), Pablo.Steinberg@mri.bund.de (P. Steinberg), S.Hampel@ifw-dresden.de (S. Hampel), Tanja.Hansen@item.fraunhofer.de (T. Hansen).

https://doi.org/10.1016/j.tiv.2019.03.028
Received 23 September 2018; Received in revised form 3 March 2019; Accepted 21 March 2019
Available online 22 March 2019

MWCNT types to identify which of them would provide the best basis for developing a MWCNT-based drug carrier system. We analyzed the cytotoxic effects of the MWCNTs in A549 human lung epithelial cells as a possible target (lung cancer) and exposure site. Additionally, we used HepG2 cells, since results of several research groups indicated that intravenously applied CNTs accumulate mostly in the liver (Deng et al., 2007; Liu et al., 2006; Liu et al., 2008b; Yang et al., 2007). To analyze the effect of the MWCNTs on cell viability/metabolic activity and membrane integrity, we performed both the WST-8 assay and the lactate dehydrogenase (LDH) assay. We additionally investigated the potential of the two MWCNT types to induce the intracellular production of ROS by using the DCFH-DA assay. Finally, we studied the effects on cell proliferation by performing a cell cycle analysis.

Based on data in the scientific literature, we predicted that the presented MWCNTs would induce toxic effects *in vitro* and therefore cannot be used for drug delivery without a further functionalization. We additionally hypothesized that the removal of iron from the MWCNT structure could potentially reduce the occurring cytotoxic effects.

2. Materials and methods

2.1. Characteristics and treatment of MWCNTs

The MWCNTs were produced using aerosol-assisted chemical vapor deposition (CVD) with cyclohexane as precursor material and ferrocene as a catalyst. The MWCNTs were divided into two groups. The first group was obtained *via* the CVD process, still containing the iron catalyst (from now on referred to as 'Fe-CNTs'). The second group (produced together with the Fe-CNTs) was heat-treated at 2600 °C for 60 min under a protective argon atmosphere to completely remove the catalyst/iron (from now on referred to as 'nonFe-CNTs'). The morphology of the MWCNTs was investigated using a scanning electron microscope (Supra 55; Zeiss, Germany). Both groups showed lengths of 16.5 ± 8 µm and diameters of 48 ± 12 nm. Fig. 1 shows the Raman spectra for both MWCNT groups. Both groups show the characteristic G-peak at 1600 cm^{-1} and a D-peak at 1300 cm^{-1}. The D-peak arises from defects on the MWCNT surface and increases with their amount. The D/G ratios suggest that the nonFe-CNTs contain significantly fewer defects compared to the Fe-CNTs (D/G ratio Fe-CNTs ~1, nonFe-CNTs < < 1).

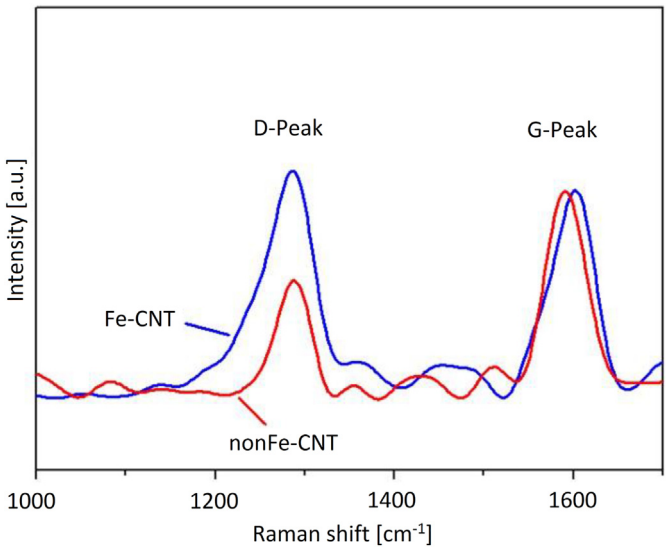

Fig. 1. Raman spectra of the 2 MWCNTs. The G-peak (1600 cm^{-1}) is a characteristic of the bulk material (graphene). The D-peak (1300^{cm-1}) is generated by defects on the CNT surface. The lower D/G ratio for the nonFe-CNTs indicates that these MWCNTs contain significantly fewer surface defects. This arises from the heat-treating procedure. (Colored version available online).

Table 1
Surface composition of the two Multi-Walled Carbon Nanotube types analyzed by X-ray photoelectron spectroscopy. [C ≡ Carbon; N ≡ Nitrogen; O_2 ≡ Oxygen].

Element	C (wt%)	N (wt%)	O_2 (wt%)
Fe-CNT	94,8	0,3	4,9
nonFe-CNT	99	0,3	< 1

The MWCNTs were sterilized in a hot air sterilizer (Memmert, Germany) at 160 °C for 4 h. For the exposure of the cells, the MWCNTs were suspended in cell culture medium containing 10% *v*/v fetal bovine serum by using an ultrasound rod (Sonopuls HD 2070; Bandelin Electronic, Germany). The MWCNT solutions were sonicated twice for 5 min in an ice bath (full power, 9/10 interval) with a short cooling interval. The dispersion of the two MWCNTs was analyzed using a scanning electron microscope (as mentioned above). The analysis revealed strongly dispersed CNTs without bundles or clusters (Fig. S1, supplement data). We also analyzed the surface composition by X-ray photoelectron spectroscopy (XPS). The XPS results are presented in Table 1. The main difference between the two MWCNT groups is the amount of oxygen (O_2) bound to the surface. The Fe-CNTs show ~5 wt % of O_2 on the surface, whereas the nonFe-CNTs show < 1 wt% because of the heat treatment under argon atmosphere. All steps until after the suspension of the MWCNTs in cell culture medium were performed while wearing a respirator class FFP3.

2.2. Cell culture and treatment

A549 lung epithelial cells (ATCC CCL-185) and HepG2 cells (ATCC HB-8065) were used in the experiments. Both cell lines were maintained in tissue culture flasks (TTP; Switzerland) using Dulbecco's modified Eagle's medium (FG 0415; Biochrom AG) supplemented with 10% v/v fetal bovine serum (S 0115; Biochrom AG) and 0.01% Gentamicin. Cells were cultivated at 37 °C and 5% CO_2 and were split upon reaching high confluence (mostly twice a week). For the experiments, cells were seeded in different well plates using 2.5 × 10^4 cells/cm^2 growth area in the case of the A549 cells and 8.5 × 10^4 cells/cm^2 in the case of the HepG2 cells. Because culture vessels with different volumes were used during the experiments, the MWCNT exposure was calculated as µg/cm^2 growth area instead of µg/ml culture volume. MWCNT concentrations of 1, 10 and 25 µg/cm^2 were used in the following experiments if not otherwise stated.

2.3. Cell viability assay (WST-8)

The Cell Counting Kit - 8 (CCK-8) (Dojindo, Germany) was used. In this test, a tetrazolium salt ((2-(2-methoxy-4-nitrophenyl)-3-(4-nitrophenyl)-5-(2,4-disulfophenyl)-2H-tetrazolium)) is reduced to formazan by viable and metabolically active cells. As a result, the amount of produced formazan is equivalent to the number of viable cells and their metabolic activity. For the experiment, cells were seeded in 24-well plates and cultivated for 48 h. After the initial cultivation, the cell culture medium was removed, and cell culture media containing MWCNTs were added to the cells. Triton X-100 (2%) was added to one group as a positive control. The cells were incubated with MWCNTs for 24 or 48 h. After that, the MWCNT-containing media were removed, and the cells were washed twice with phosphate-buffered saline (PBS). Six hundred microliters culture medium containing 10% CCK-8 solution was added to each well and the well plates were incubated for 2 h at 37 °C and 5% CO_2. Then, the medium was filtered by using a 0.2 µm syringe filter (Filtropour S 0.2 µm; Sarstedt, Germany) to remove all MWCNTs before the analysis. The formazan content was measured using an UV/VIS spectrometer at 450 nm (EPOCH Reader, BioTek, Germany).

2.4. Membrane integrity (LDH) assay

For the quantification of the LDH leakage from damaged cells the Cytotoxicity Detection Kit (LDH) (Roche Applied Science, Germany) was used. An increased LDH leakage from exposed cells into the surrounding culture medium is an indication of cell membrane damage. Additionally, LDH values can be used to calculate the percentage of cytotoxicity in the cell culture induced by the test material. For this purpose, cells were seeded in 24-well plates and exposed for 24 or 48 h as described above. Triton X-100 (2%) was used as a positive control to achieve a maximum LDH release. After the exposure period, the culture medium was filtered into Eppendorf cups using syringe filters (see above). One hundred microliters of each filtrate were added to a new 96-well plate. One hundred microliters of the prepared assay solution were added to each well and the well plates were incubated for 30 min on a shaker (at low speed, protected from light, at room temperature). After the incubation, LDH levels were measured using an ELISA plate reader (EPOCH Reader, BioTek, Germany) at 490 nm.

2.5. Measurement of the intracellular ROS production

The 2,7-dichlorodihydrofluorescein diacetate (DCFH-DA) assay was performed to determine the ROS levels formed intracellularly after exposure of the cells to the two MWCNT types. DCFH-DA is a dye molecule that can pass through the lipid membrane and is reduced to DCFH by esterase. Coming into contact with ROS such as $OH\cdot$ or $O_2\cdot$, DCFH is converted to the fluorescent molecule DCF. The fluorescence intensity measured for each cell *via* flow cytometry is proportional to the amount of ROS generated inside the cell. For our experiments, the cells were seeded in 6-well plates and exposed to 1 and 10 µg/cm^2 of each MWCNT as described above. Paraquat was used as a positive control (5 mM for a 24 h exposure and 3 mM for a 48 h exposure) to induce a strong ROS production. After treatment, the exposure media were removed, and the cells were washed twice with PBS. Fresh culture medium containing 1 mg/ml DCFH-DA dissolved in DMSO was added to each well and the plates were incubated for 30 min. The medium was removed and the cells were washed twice with PBS before being detached with Trypsin/EDTA solution and transferred into Falcon tubes. To remove the remaining MWCNTs the cell solutions were centrifuged at 800 rpm for 5 min and resuspended in fresh culture medium. This step was repeated twice. After the third centrifugation, the cells were resuspended in PBS. 10 µl Propidium iodide (PI) was added, and each sample was filtered through a 35 µm filter mesh into flow cytometry activated cell sorter (FACS) tubes.

To balance the benefit of strong MWCNT removal and the disadvantage of exposing the cells to mechanical stress, the number of centrifugation and resuspension steps was limited to three. The samples were analyzed using a flow cytometer (FACScan, Becton Dickinson, Germany).

2.6. Cell cycle analysis

To investigate the effect of MWCNT exposure on cell proliferation, the cell cycle of the exposed cells was analyzed. The cell cycle state can be determined by measuring the DNA content in a cell. A normal DNA level represents cells in the G0/1 phase (gap phase), whereas a doubled DNA content represents cells in the G2/M phase. Each cell with a DNA content between normal and double is deemed to be in the S phase (synthesis). The CycleTEST™ Plus - DNA Reagent Kit (Becton Dickinson, Germany) was used for the analysis. Briefly, the cell membrane is permeabilized using a trypsin buffer and RNA in the cells is removed using ribonuclease A. Finally, PI, which binds to DNA, is added. The amount of DNA-bound PI, which is proportional to the DNA content, is measured by flow cytometry. Cells were seeded in 6-well plates as described above. After 24 h, the cells were exposed to the two MWCNT types at concentrations of 0.5, 1 and 5 µg/cm^2 for 24 h. Thereafter, the exposure medium was removed, and each well was washed twice using PBS. The cells were detached from the plates and transferred into Falcon tubes. Finally, the samples were filtered into FACS tubes by using a 35 µm filter mash. A flow cytometer (FACScan, Becton Dickinson) was used for data collection. The data was analyzed using the software 'ModFit LT for Win32' (version 3.3.11). This analysis was performed solely after 24 h of exposure to avoid increased cell death over a prolonged exposure period. The goal was to investigate the possibility of a cell cycle interference provoked by the MWCNTs in general and not a possible time-dependency.

2.7. Statistical analysis

Experimental data are expressed as mean ± standard deviation (SD). The statistical significance of differences between the experimental groups, each of them consisting of data from ≥3 individual experiments, was determined by one-way analysis of variance (ANOVA) and Bonferroni post-test using the GraphPad Prism 4 (GPP) software. *P* values < .05 were considered statistically significant.

3. Results

3.1. Cell viability assay (WST-8)

To assess the viability of cells exposed to Fe- and nonFe-CNTs, the WST-8 assay was performed. Both cell lines showed a significant, dose-

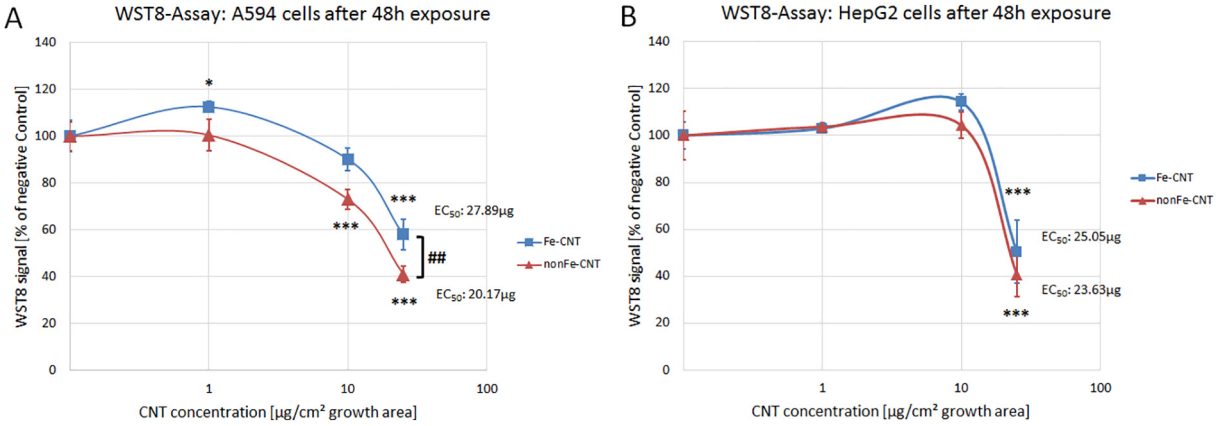

Fig. 2. Effect of Fe- and nonFe-CNTs on the viability of A549 (A) and HepG2 cells (B) after a 48 h exposure. The asterisks indicate statistically significant differences between the MWCNT-exposed cells and the negative controls: * ≡ $p < .05$, ** ≡ $p < .01$, *** ≡ $p < .001$; # indicates statistically significant differences between the two MWCNT types: # ≡ $p < .05$, ## ≡ $p < .01$, ### ≡ $p < .001$; EC_{50} = Half maximal effective concentration. (Colored version available online).

dependent decrease in cell viability after a 48 h exposure to both MWCNTs (Fig. 2). When compared to the results after 24 h (Fig. S2, supplement data), the effects were also time-dependent. In the case of the A549 lung epithelial cells (Fig. 2A), Fe-CNTs decreased the cell viability significantly only at the high concentration of 25 μg/cm^2. In contrast, the nonFe-CNTs led to a significant cell viability decrease at concentrations of 10 and 25 μg/cm^2. Moreover, the reduction in cell viability at both 10 and 25 μg/cm^2 was significantly stronger when compared to that after exposure to the Fe-CNTs, which is in line with the significantly lower half maximal effective concentration (EC_{50}) of the nonFe-CNTs (20.2 μg/cm^2) if compared to the Fe-CNTs (27.9 μg/cm^2). The HepG2 cells showed a hysteresis reaction after a 24 h exposure to the MWCNTs over the entire dose range (Fig. S2B, supplement data). After 48 h of exposure, both MWCNTs showed a strong, significant reduction of cell viability at the high concentration of 25 μg/cm^2. The nonFe-CNTs showed a slightly but not significantly stronger viability decrease. This tendency is also reflected in the EC_{50}-values, which were lower in the case of the nonFe-CNTs (23.6 μg/cm^2) as compared to the Fe-CNTs (25.0 μg/cm^2).

3.2. Membrane integrity assay (LDH)

To substantiate the findings from the cell viability analysis, the LDH assay was performed. The results for both cell lines after a 48 h exposure to each MWCNT are presented in Fig. 3. In the case of the A549 lung epithelial cells (Fig. 3A), the Fe-CNTs showed a significant increase in LDH release over the whole concentration range (up to 300% of the negative control). In the case of the nonFe-CNTs, the LDH release was significantly increased up to 550% when compared to the negative control. The LDH release after exposure to the nonFe-CNTs is significantly higher compared to the Fe-CNTs at either 10 or 25 μg/cm^2. A difference between the two MWCNTs was also observed after 24 h of exposure, though it was not statistically significant (p = .069). In this case, only the nonFe-CNTs led to an increase (175%) in the LDH leakage (Fig. S3A, supplement data). Likewise, exposing the HepG2 cells to both MWCNTs at concentrations of 10 and 25 μg/cm^2 for 48 h led to a significant increase in LDH release. The total amount of LDH released by the HepG2 cells was substantially lower if compared to that released by the A549 cells (200% *vs.* 550%), and no significant difference was detected between the nonFe-CNTs and the Fe-CNTs. The 24 h exposure (Fig. S3B, supplement data) showed only a marginal, not significant increase in LDH release by the HepG2 cells.

3.3. Measurement of the intracellular ROS production

The intracellularly produced ROS were quantified by performing the DCFH-DA assay. The maximum MWCNT concentration was decreased from 25 to 10 μg/cm^2 to ensure a sufficient CNT removal from the cell suspension, with a limited number of three centrifugation and resuspension steps. Results are shown after 24 h of exposure (results after 48 h are indicated in the supplement data) because of the short-lived nature and time-dependent occurrence of ROS (Nathan and Cunningham-Bussel, 2013). Fig. 4 shows the results for both cell lines after 24 h of MWCNT exposure. In both cell lines, the production of ROS was significantly increased when the cells were exposed to the nonFe-CNTs at a concentration of 10 μg/cm^2, whereas in the case of the Fe-CNTs no significant increase in ROS production was observed. In the case of the A549 cells (Fig. 4A), the difference between the two MWCNT types is statistically significant. After 48 h of exposure (Fig. S4, supplement data), the nonFe-CNTs led to a significant increase in ROS production in both cell lines at a concentration of 10 μg/cm^2.

3.4. Cell cycle analysis

The CycleTEST™ Plus assay was utilized to examine the effects of the MWCNTs on the cell cycle and, hence, the cell proliferation. This experiment was not conducted with the HepG2 cells because these cells are polynuclear. The results in the case of the A549 lung epithelial cells exposed to the Fe- and nonFe-CNTs are shown in Fig. 5. The Fe-CNTs did not induce significant changes in the cell cycle distribution of the cells except for a slight decrease in the percentage of cells in the G0/G1 phase (Fig. 5A). In contrast, exposure to the nonFe-CNTs led to significant changes in the cell cycle distribution of A549 cells when compared to the negative control. In the case of the 1 and 5 μg/cm^2 concentrations, the percentage of cells in the S phase was significantly decreased, while the amount of cells in the G2 phase was significantly and dose-dependently increased. An increase in the percentage of cells being in the G2 phase would normally indicate an increased cell proliferation. However, an increased proliferation would also result in an increased cell number in the S phase (see 'Discussion'). Fig. 5C and D show raw data from the flow cytometry analysis, in which the significant changes under the influence of 5 μg/cm^2 nonFe-CNTs, compared to the negative control, are exemplarily shown.

4. Discussion

The cytotoxicity of two different MWCNT types, one with and one without residual iron, were tested. Post-production removal of the iron

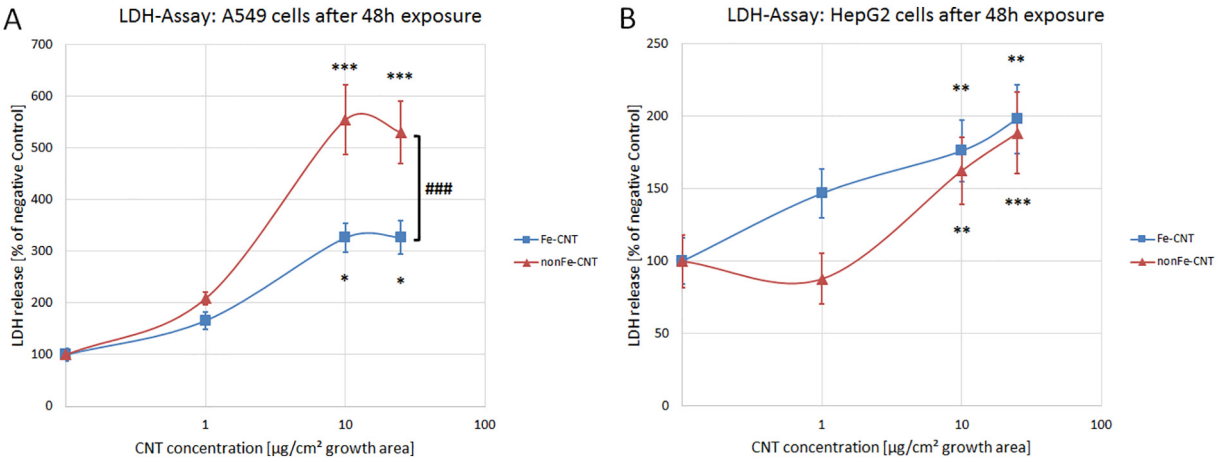

Fig. 3. Effect of Fe- and nonFe-CNTs on LDH leakage in A549 (A) and HepG2 cells (B) after a 48 h exposure. Asterisks indicate statistically significant differences between the MWCNT-exposed cells and the negative controls: * ≡ p < .05, ** ≡ p < .01, *** ≡ p < .001; # indicates statistically significant differences between the two MWCNT types # ≡ p < .05, ## ≡ p < .01, ### ≡ p < .001. (Colored version available online).

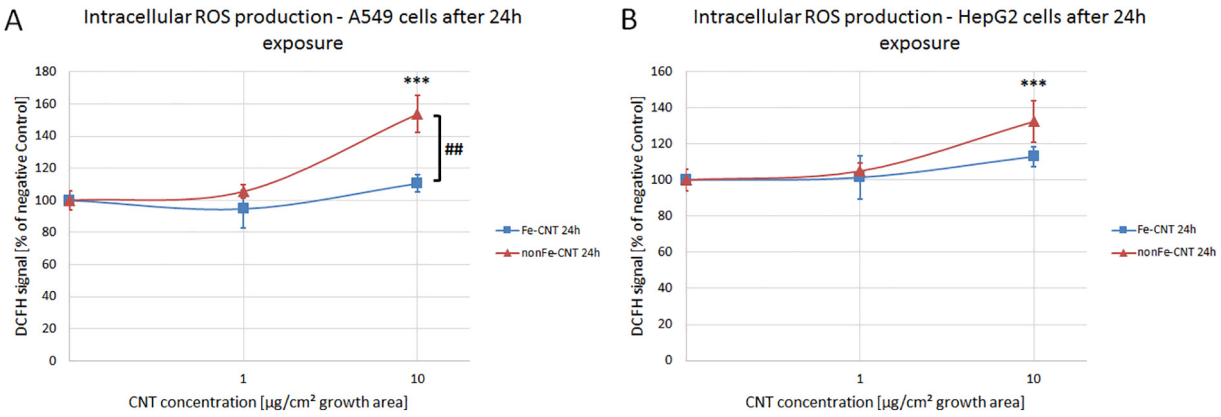

Fig. 4. Effect of Fe- and nonFe-CNTs on ROS production in A549 (A) and HepG2 cells (B) after a 24 h exposure. Asterisks indicate statistically significant differences between the MWCNT-exposed cells and the negative controls: * ≡ $p < .05$, ** ≡ $p < .01$, *** ≡ $p < .001$; # indicates statistically significant differences between the two MWCNT types # ≡ p < .05, ## ≡ p < .01, ### ≡ $p < .001$. (Colored version available online).

catalyst resulted in significantly fewer surface defects (nonFe-CNTs). We hypothesized that both MWCNTs would exhibit cytotoxic effects, which may potentially be increased by the remaining iron. Adverse effects would most likely be a reduction in metabolic activity/viability, damage to the lipid membrane, the production of ROS and interference with the cell cycle/cell proliferation.

The diameter, length, surface composition and Raman spectra of the MWCNTs were characterized. After the heat treatment, the length and diameter of the MWCNTs were identical to those of the untreated group. The Raman spectra and data on the surface composition point

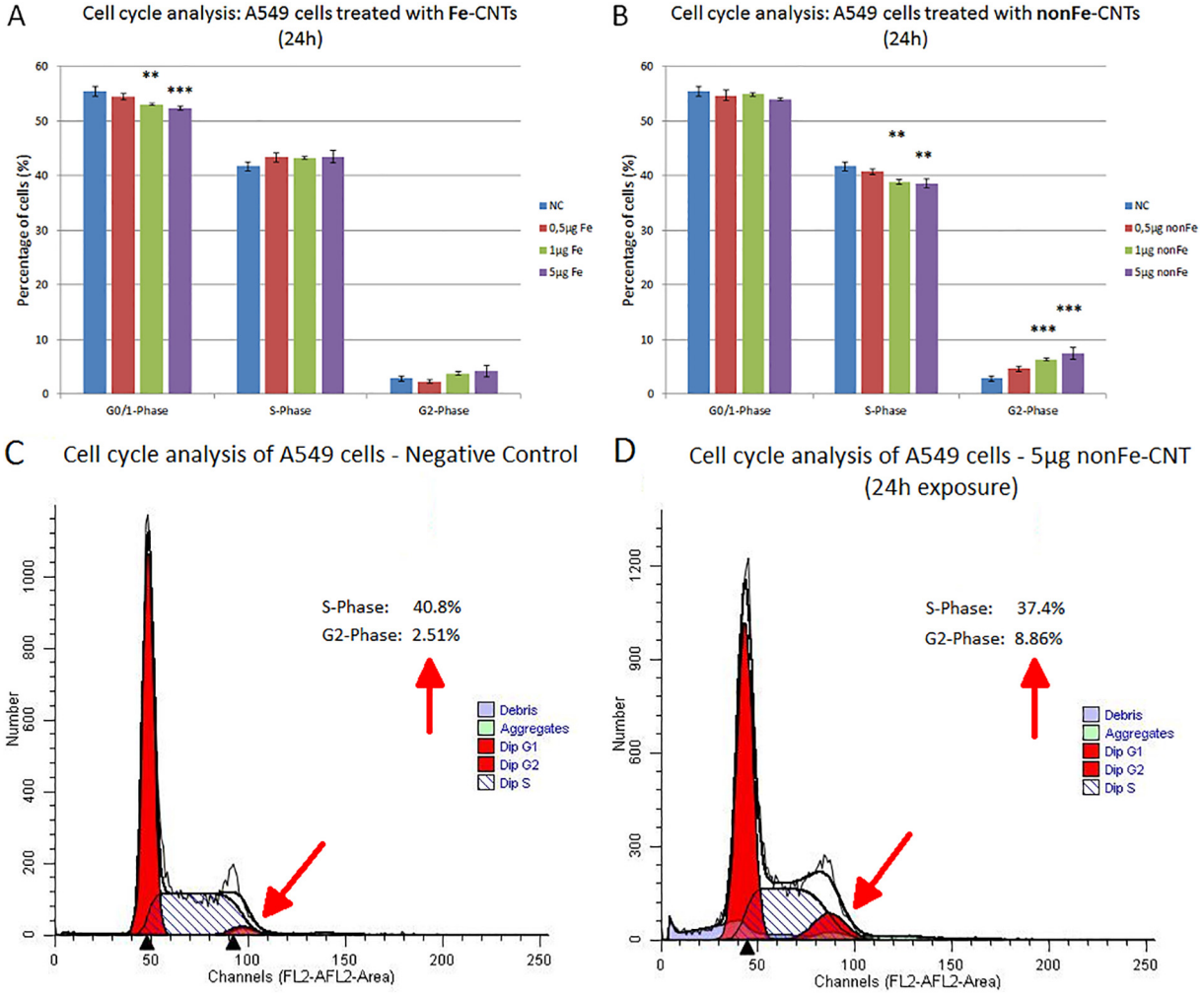

Fig. 5. Effect of Fe- and nonFe-CNTs on the cell cycle distribution of A549 (A) and HepG2 cells (B). Raw flow cytometry data in the case of a negative control and cells exposed to 5 µg/cm^2 nonFe-CNTs are shown in (C) and (D), respectively. The arrows point out to the number of cells in the G2 phase, and the percentage of cells in the G2 and S phases are indicated. Asterisks indicate statistically significant differences between the CNT-exposed cells and the negative controls: * ≡ $p < .05$, ** ≡ $p < .01$, *** ≡ $p < .001$. (Colored version available online).

out that the nonFe-CNTs contain fewer surface defects and less O_2 bound to their surface. Due to the production method, the remaining iron catalyst, which initially acted as a growth seed, is encapsulated within the Fe-CNT core. This is indicated by the absence of iron in the XPS surface analysis.

Even though CNTs have been shown to interfere with some commonly used cell viability assays (Casey et al., 2007; Wörle-Knirsch, Pulskamp, and Krug, 2006), no interference was reported for the WST-8 cell viability assay. Using this assay, we showed that the cell viability of A549 lung epithelial cells and HepG2 cells were significantly reduced in a time- and dose-dependent manner after exposure to both MWCNT types. After a 24 and 48 h exposure period, the nonFe-CNTs led to a significantly stronger decrease in viability/metabolic activity in A549 cells if compared to the Fe-CNTs. Time- and dose-dependent cytotoxic effects of MWCNTs on various cell lines, including A549 cells, has also been reported by several research groups in the past (Guo, Zhang, Zheng, Yang, and Zhu, 2011; Han, Xu, Li, Ren, and Yang, 2012; Simon-Deckers et al., 2008; Ursini et al., 2012).

The LDH assay revealed a significant leakage of LDH, following membrane damage, after the exposure of the A549 and HepG2 cells to both types of MWCNTs. However, especially in the case of the A549 cells, the membrane damage was significantly stronger after exposure to the nonFe-CNTs. It is probable that this directly results from the lack of surface defects in the case of the nonFe-CNTs. An increased amount of surface defects results in a reduced amount of delocalized electrons on the CNT surface. Contrariwise, fewer defects result in many delocalized electrons, which lead to an increase in hydrophobicity, leading to an increase in binding and damaging of hydrophobic structures such as lipid membranes. Subsequently, the increased membrane damage results in an increased cytotoxicity when cells were exposed to the nonFe-CNTs. As we proposed, membrane damage was expected, since an increased leakage of LDH following exposure to MWCNTs in A549 cells and other cell lines had been reported by several other research groups (Chen et al., 2011; Reddy, Reddy, Krishna, and Himabindu, 2010; Ursini et al., 2012).

Based on the physical and chemical properties of the MWCNTs, it could be expected that an increased number of delocalized electrons on their surface and, hence, an increased hydrophobicity could lead to an enhanced formation of ROS. This in turn could be attributed to an inductive effect as a result of a dense electron cloud. Our data using the DCFH-DA assay showed that 10 μg/cm^2 nonFe-CNTs led to a significantly increased intracellular production of ROS following a 24 and 48 h exposure, whereas the Fe-CNTs showed no increased radical formation. The increased production of ROS and the increase in oxidative stress following MWCNT exposure was also reported for various cell lines, including A549 and HepG2 cells, by several other research groups (Chen et al., 2011; Kermanizadeh et al., 2013; Reddy, Reddy, Krishna, and Himabindu, 2010; Shvedova et al., 2003; Yang, Liu, Yang, Zhang, and Xi, 2009).

The ability of CNTs to cross cell membranes, both by active and passive transport processes, has previously been reported in the scientific literature (Bianco, Kostarelos, and Prato, 2005; Kateb et al., 2007; Prato, Kostarelos, and Bianco, 2007). The passive penetration due to their needle-like appearance suggests that both SWCNTs and low diameter MWCNTs could enter and accumulate inside cells and interfere with various components of the cells including DNA in the nucleus, the cytoskeleton or other organelles. To investigate the effects of the MWCNTs on cell proliferation and the cell cycle distribution, we performed a cell cycle analysis at relatively low concentrations (*i.e.* 0.5, 1 and 5 μg/cm^2). In A549 cells, the nonFe-CNTs led to a significantly increased percentage of cells in the G2/M phase, while the percentage of cells in the S phase was significantly reduced at concentrations of 3 and 5 μg/cm^2 and a 24 h exposure period. These results point to a G2 phase arrest induced by the MWCNTs. The MWCNTs migrate into the nucleus and destroy the spindle apparatus at the beginning of the mitosis. Since the spindle apparatus is shattered into multiple pieces, more than two spindle poles are created. As a result, the chromosomes cannot be separated during mitosis, which results in an arrest of the cells in the G2/M phase. This effect has been reported by various other research groups in the case of both SW- and MWCNTs in different cell lines (Hampel et al., 2008; Sargent et al., 2009; Sargent et al., 2011; Wang, Sun, Bao, Liu, and An, 2010). The described effect results in reduced cell proliferation, cell death by apoptosis and the possible induction of aneuploidy if apoptosis does not occur.

Our initial aim was to investigate whether the residual iron (Fe-CNT) from the production process could cause increased cytotoxic effects and therefore if the heat-treated MWCNTs (nonFe-CNTs) should be favored as a drug carrier base material. Our results show that the heat treatment results in a significantly increased cytotoxicity, including increased radical formation and cell cycle interference. Since the two MWCNT types, according to our characterization, only differ in the amount of surface defects and surface bound O_2 we conclude that the lack of surface defects results in increased cytotoxicity. Obviously, the residual iron does not enhance the observed cytotoxic effects or only to a substantially smaller extent than the altered surface structure. It is an interesting finding that significant differences in the cytotoxic potential of the two MWCNT types were mainly observed in A549 cells, indicating a higher sensitivity of this cell line to CNT exposure compared to HepG2 cells. Our initial goal was to investigate if the heat-treatment changes the cytotoxicity of the MWCNTs and which CNT type would provide the best basis for the development of an MWCNT-based drug carrier system. Our results indicate that the heat-treatment increases the MWCNTs cytotoxicity. Based on the results, we conclude that the untreated MWCNTs are a more promising basis for the development of *in vivo* applications, like for example drug carrier systems, since their cytotoxicity was significantly lower compared to the heat-treated MWCNTs. However, the observed cytotoxicity demands a functionalization of the MWCNTs to achieve biocompatibility before a potential *in vivo* application. This could be achieved for example by PEGylation (Dumortier et al., 2006; Sayes et al., 2005; Schipper et al., 2008).

Acknowledgements

We thank Dr. Anja Hackbarth (Fraunhofer Institute for Toxicology and Experimental Medicine, Hannover, Germany) for the SEM analysis of the MWCNTs.

Appendix A. Supplementary data

Supplementary data to this article can be found online at https://doi.org/10.1016/j.tiv.2019.03.028.

References

Ahn, J.-H., Kim, H.-S., Lee, K.J., Jeon, S., Kang, S.J., Sun, Y., Nuzzo, R.G., Rogers, J.A., 2006. Heterogeneous three-dimensional electronics by use of printed semiconductor nanomaterials. Science 314 (5806), 1754–1757.

Aldieri, E., Fenoglio, I., Cesano, F., Gazzano, E., Gulino, G., Scarano, D., Attanasio, A., Mazzucco, G., Ghigo, D., Fubini, B., 2013. The role of iron impurities in the toxic effects exerted by short multiwalled carbon nanotubes (MWCNT) in murine alveolar macrophages. J. Toxic. Environ. Health A 76 (18), 1056–1071.

Bianco, A., Kostarelos, K., Prato, M., 2005. Applications of carbon nanotubes in drug delivery. Curr. Opin. Chem. Biol. 9 (6), 674–679.

Casey, A., Herzog, E., Davoren, M., Lyng, F.M., Byrne, H.J., Chambers, G., 2007. Spectroscopic analysis confirms the interactions between single walled carbon nanotubes and various dyes commonly used to assess cytotoxicity. Carbon 45, 1425–1432.

Chen, B., Liu, Y., Song, W.M., Hayashi, Y., Ding, X.C., Li, W.H., 2011. In vitro evaluation of cytotoxicity and oxidative stress induced by multiwalled carbon nanotubes in murine RAW 264.7 macrophages and human A549 lung cells. Biomed. Environ. Sci. 24 (6), 593–601.

De Jong, W.H., Borm, P.J., 2008. Drug delivery and nanoparticles:applications and hazards. Int. J. Nanomedicine 3 (2), 133–149.

Deng, X., Jia, G., Wang, H., Sun, H., Wang, X., Yang, S., Wang, T., Liu, Y., 2007. Translocation and fate of multi-walled carbon nanotubes in vivo. Carbon 45 (7), 1419–1424.

Dumortier, H., Lacotte, S., Pastorin, G., Marega, R., Wu, W., Bonifazi, D., Briand, J.P.,

Prato, M., Muller, S., Bianco, A., 2006. Functionalized carbon nanotubes are non-cytotoxic and preserve the functionality of primary immune cells. Nano Lett. 6 (7), 1522–1528.
Guo, Y., Zhang, J., Zheng, Y., Yang, J., Zhu, X., 2011. Cytotoxic and genotoxic effects of multi-wall carbon nanotubes on human umbilical vein endothelial cells in vitro. Mutat. Res. Genet. Toxicol. Environ. Mutagen. 721, 184–191.
Hampel, S., Kunze, D., Haase, D., Kramer, K., Rauschenbach, M., Ritschel, M., Leonhardt, A., Thomas, J., Oswald, S., Hoffmann, V., Buchner, B., 2008. Carbon nanotubes filled with a chemotherapeutic agent: a nanocarrier mediates inhibition of tumor cell growth. Nanomedicine (London) 3 (2), 175–182.
Han, Y., Xu, J., Li, Z., Ren, G., Yang, Z., 2012. In vitro toxicity of multi-walled carbon nanotubes in C6 rat glioma cells. NeuroToxicology 33, 1128–1134.
Holsapple, M.P., Farland, W.H., Landry, T.D., Monteiro-Riviere, N.A., Carter, J.M., Walker, N.J., Thomas, K.V., 2005. Research strategies for safety evaluation of nanomaterials, part II: toxicological and safety evaluation of nanomaterials, current challenges and data needs. Toxicol. Sci. 88 (1), 12–17.
Kagan, V.E., Tyurina, Y.Y., Tyurin, V.A., Konduru, N.V., Potapovich, A.I., Osipov, A.N., Kisin, E.R., Schwegler-Berry, D., Mercer, R., Castranova, V., Shvedova, A.A., 2006. Direct and indirect effects of single walled carbon nanotubes on RAW 264.7 macrophages: role of iron. Toxicol. Lett. 165 (1), 88–100.
Kateb, B., Van Handel, M., Zhang, L., Bronikowski, M., Manohara, H., Badie, B., 2007. Internalization of MWCNTs by microglia: possible application in immunotherapy of brain tumors. NeuroImage 37, S9–S17.
Kermanizadeh, A., Vranic, S., Boland, S., Moreau, K., Baeza-Squiban, A., Gaiser, B.K., Andrzejczuk, L.A., Stone, V., 2013. An in vitro assessment of panel of engineered nanomaterials using a human renal cell line: cytotoxicity, pro-inflammatory response, oxidative stress and genotoxicity. BMC Nephrol. 14, 96.
Leonhardt, A., Hampel, S., Müller, C., Mönch, I., Koseva, R., Ritschel, M., Elefant, D., Biedermann, K., Büchner, B., 2006. Synthesis, properties, and applications of ferromagnetic-filled carbon nanotubes. Chem. Vap. Depos. 12 (6), 380–387.
Liu, Z., Cai, W., He, L., Nakayama, N., Chen, K., Sun, X., Chen, X., Dai, H., 2006. In vivo biodistribution and highly efficient tumour targeting of carbon nanotubes in mice. Nat. Nanotechnol. 2, 47–52.
Liu, Z., Chen, K., Davis, C., Sherlock, S., Cao, Q., Chen, X., Dai, H., 2008a. Experimental therapeutics, molecular targets, and chemical biology: drug delivery with carbon nanotubes for in vivo cancer treatment. Cancer Res. 68, 6652–6660.
Liu, Z., Davis, C., Cai, W., He, L., Chen, X., Dai, H., 2008b. Circulation and long-term fate of functionalized, biocompatible single-walled carbon nanotubes in mice probed by Raman spectroscopy. Proc. Natl. Acad. Sci. U. S. A. 105 (5), 1410–1415.
Miyagawa, H., Misra, M., Mohanty, A.K., 2005. Mechanical properties of carbon nanotubes and their polymer nanocomposites. J. Nanosci. Nanotechnol. 5 (10), 1593–1615.
Moisala, A., Nasibulin, A.G., Brown, D.P., Jiang, H., Khriachtchev, L., Kauppinen, E.I., 2006. Single-walled carbon nanotube synthesis using ferrocene and iron pentacarbonyl in a laminar flow reactor. Chem. Eng. Sci. 61 (13), 4393–4402.
Monteiro-Riviere, N.A., Nemanich, R.J., Inman, A.O., Wang, Y.Y., Riviere, J.E., 2005. Multi-walled carbon nanotube interactions with human epidermal keratinocytes. Toxicol. Lett. 155 (3), 377–384.
Nathan, C., Cunningham-Bussel, A., 2013. Beyond oxidative stress: an immunologist's guide to reactive oxygen species. Nat. Rev. Immunol. 13 (5), 349–361.
Oberdorster, G., Oberdorster, E., Oberdorster, J., 2005a. Nanotoxicology: an emerging discipline evolving from studies of ultrafine particles. Environ. Health Perspect. 113 (7), 823–839.
Oberdorster, G., Maynard, A., Donaldson, K., Castranova, V., Fitzpatrick, J., Ausman, K., Carter, J., Karn, B., Kreyling, W., Lai, D., Olin, S., Monteiro-Riviere, N., Warheit, D., Yang, H., ILSI Research Foundation, A. r. f. t, 2005b. Principles for characterizing the potential human health effects from exposure to nanomaterials: elements of a screening strategy. Part. Fibre Toxicol. 2 (8).
Prato, M., Kostarelos, K., Bianco, A., 2007. Functionalized carbon nanotubes in drug design and discovery. Acc. Chem. Res. 41 (1), 60–68.
Reddy, A.R., Reddy, Y.N., Krishna, D.R., Himabindu, V., 2010. Multi wall carbon nanotubes induce oxidative stress and cytotoxicity in human embryonic kidney (HEK293) cells. Toxicology 272 (1–3), 11–16.
Salata, O.V., 2004. Applications of nanoparticles in biology and medicine. J. Nanobiotechnol. 2 (3).
Sargent, L.M., Shvedova, A.A., Hubbs, A.F., Salisbury, J.L., Benkovic, S.A., Kashon, M.L., Lowry, D.T., Murray, A.R., Kisin, E.R., Friend, S., McKinstry, K.T., Batelli, L., Reynolds, S.H., 2009. Induction of aneuploidy by single-walled carbon nanotubes. Environ. Mol. Mutagen. 50 (8), 708–717.
Sargent, L.M., Hubbs, A.F., Young, S.-H., Kashon, M., Dinu, C.Z., Salisbury, J.L., Benkovic, S.A., Lowry, D.T., Murray, A.R., Kisin, E.R., Siegrist, K.J., Batelli, L., Mastovich, J., Sturgeon, J.L., Bunker, K.L., Shvedova, A.A., Reynolds, S.H., 2011. Single-walled carbon nanotube-induced mitotic disruption. Mutat. Res. Genet. Toxicol. Environ. Mutagen. 745 (1–2), 28–37.
Sayes, C.M., Liang, F., Hudson, J.L., Mendez, J., Guo, W., Beach, J.M., Moore, V.C., Doyle, C.D., West, J.L., Billups, W.E., Ausman, K.D., Colvin, V.L., 2005. Functionalization density dependence of single-walled carbon nanotubes cytotoxicity in vitro. Toxicol. Lett. 161 (2), 135–142.
Schipper, M.L., Nakayama-Ratchford, N., Davis, C.R., Kam, N.W.S., Chu, P., Liu, Z., Sun, X., Dai, H., Gambhir, S.S., 2008. A pilot toxicology study of single-walled carbon nanotubes in a small sample of mice. Nat. Nanotechnol. 3, 216–221.
Shvedova, A.A., Castranova, V., Kisin, E.R., Schwegler-Berry, D., Murray, A.R., Gandelsman, V.Z., Maynard, A., Baron, P., 2003. Exposure to carbon nanotube material: assessment of nanotube cytotoxicity using human keratinocyte cells. J. Toxicol. Environ Health A 66 (20), 1909–1926.
Simon-Deckers, A., Gouget, B., Mayne-L'Hermite, M., Herlin-Boime, N., Reynaud, C., Carriere, M., 2008. In vitro investigation of oxide nanoparticle and carbon nanotubes toxicity and intracellular accumulation in A549 human pneumocytes. Toxicology 253, 137–146.
Stern, S.T., McNeil, S.E., 2007. Nanotechnology safety concerns revisited. Toxicol. Sci. 101 (1), 4–21.
Ursini, C.L., Cavallo, D., Fresegna, A.M., Ciervo, A., Maiello, R., Buresti, G., Casciardi, S., Tombolini, F., Bellucci, S., Iavicoli, S., 2012. Comparative cyto-genotoxicity assessment of functionalized and pristine multiwalled carbon nanotubes on human lung epithelial cells. Toxicol. in Vitro 26 (6), 831–840.
Verma, S., Domb, A.J., Kumar, N., 2011. Nanomaterials for regenerative medicine. Nanomedicine (London) 6 (1), 157–181.
Visalli, G., Facciolà, A., Iannazzo, D., Piperno, A., Pistone, A., Di Pietro, A., 2017. The role of the iron catalyst in the toxicity of multi-walled carbon nanotubes (MWCNTs). J. Trace Elem. Med. Biol. 43, 153–160.
Wang, J., Sun, P., Bao, Y., Liu, J., An, L., 2010. Cytotoxicity of single-walled carbon nanotubes on PC12 cells. Toxicol. in Vitro 25, 242–250.
Wolinsky, H., 2006. Nanoregulation: a recent scare involving nanotech products reveals that the technology is not yet properly regulated. EMBO Rep. 7 (9), 858–861.
Wörle-Knirsch, J.M., Pulskamp, K., Krug, H.F., 2006. Oops they did it again! carbon nanotubes hoax scientists in viability assays. Nano Lett. 6 (6), 1261–1268.
Yang, S., Guo, W., Lin, Y., Deng, X., Wang, H., Sun, H., Liu, Y., Wang, X., Wang, W., Chen, M., Huang, Y., Sun, Y., 2007. Biodistribution of pristine single-walled carbon nanotubes in vivo. J. Phys. Chem. C 111 (48), 17761–17764.
Yang, H., Liu, C., Yang, D., Zhang, H., Xi, Z., 2009. Comparative study of cytotoxicity, oxidative stress and genotoxicity induced by four typical nanomaterials: the role of particle size, shape and composition. J. Appl. Toxicol. 29 (1), 69–78.
Zhang, L., Webster, T.J., 2008. Nanotechnology and nanomaterials: promises for improved tissue regeneration. Nano Today 4 (1), 66–80.